Fourier-transform-spectroscopy measurements in the spectra of neutral lithium, ^{6}Li I and ^{7}Li I (Li I)

Leon J. Radziemski
Department of Physics, Washington State University, Pullman, Washington 99164-2814

Rolf Engleman, Jr.
Chemistry Department, University of New Mexico, Albuquerque, New Mexico 87131

James W. Brault
University of Colorado, Cooperative Institute for Research in Environmental Science/National Oceanic and Atmospheric Administration, Boulder, Colorado 80309

(Received 24 July 1995)

The most recent measurements leading to improved Li I energy levels appeared in the late 1950s. Since then, many high- and ultrahigh-precision spectroscopy techniques have been used to measure the fine and hyperfine structures and isotope shifts of this atom. Most previous measurements were made on ^{7}Li. Using high- and low-current hollow cathode sources and Fourier-transform spectrometry, we have made measurements in both ^{7}Li and ^{6}Li including nine previously unmeasured infrared lines. Wave-number measurements were obtained on 34 lines from 1829 to 30 925 cm^{-1}. The strongest lines have been determined to ± 0.0010 cm^{-1}. We also measured 22 new isotope shifts, and added specific mass shifts for five levels. The resonance lines at 6707 Å in both isotopes, emitted by low-current, commercial lithium hollow cathode sources, were measured to ± 0.0005 cm^{-1}. The energy levels have been recalculated using the new data.

PACS number(s): 32.30.Jc

I. INTRODUCTION

The simple one-electron spectrum of neutral lithium continues to interest theorists and experimentalists. Recently there have been precise theoretical calculations of properties of the ground state, low-lying excited states, and Rydberg states [1–3]. The 670-nm $D1$ and $D2$ resonance lines are widely used in spectrochemistry and solar [4] and stellar [5] astronomy. In the latter case, they are used to determine the ^{6}Li:^{7}Li ratio, an important parameter in models of stellar evolution. Since the field shift contribution to the isotope shift between ^{6}Li and ^{7}Li is negligible, this case has been used as a test for the accuracy of specific mass shift calculations [6,7]. The perturbation of lithium levels by Stark effect yields useful information on hyperfine structure [8] and other properties.

The most recent measurements leading to improved Li I energy levels were published in the 1940s [9] and 1950s [10]. Since then many high- and ultrahigh-precision spectroscopy techniques have been used to measure the fine and hyperfine structure and isotope shift intervals of this atom. However, with the exception of a few laser-based results, no new wave-number values were measured. Using the 1-m Fourier-transform spectrometer (FTS) operated by the National Solar Observatory (NSO) at Kitt Peak, we made new measurements on both ^{6}Li and ^{7}Li, the former not having been studied in detail before.

The general structure of the one-electron spectrum of neutral lithium is shown in Fig. 1. We have observed lines in the region 1829–30 925 cm^{-1}. Levels generated from simultaneous excitation of more than one electron have been observed by others to 540 000 cm^{-1} [11], but are not included in our discussion.

II. PREVIOUS RESULTS

A. Conventional grating and interferometric spectroscopy

Spectroscopic measurements in the spectrum of neutral lithium date back to the early 1900s [12,13]. A compilation

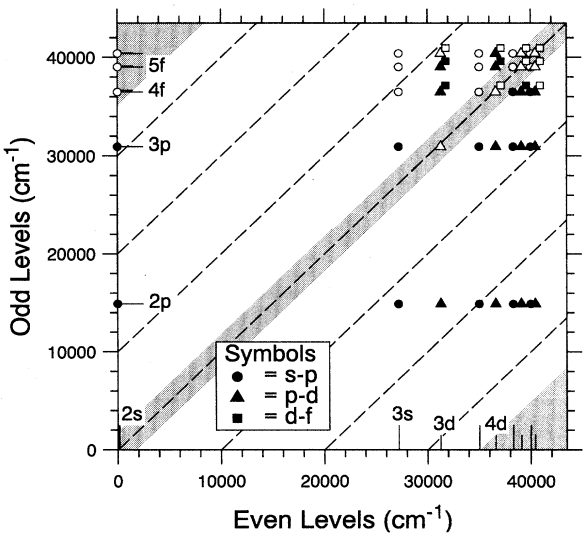

FIG. 1. The allowed transitions and levels of Li I through $n=6$ (g terms not included and only the first two of each term series labeled). Full scale on both axes is the ionization energy. Solid symbols represent transitions observed in the present study. Shaded areas in the deep UV and far IR were inaccessible to our study. The diagonal lines are lines of constant wave-number difference. The five transitions have been displaced slightly (500 cm^{-1} upward and to the left) for clarity.

of energy level values based on important early work was published in Ref. [14]. Those level values were based on the high-precision measurements of the $2s$-$2p$ and $2p$-nd ($n=3$ to 6) transitions by Meissner, Mundie, and Stelson [9]. Those measurements were later corrected by Johansson [10] using a new air refraction formula. He also measured 23 infrared lines with a grating spectrometer (accuracy of ± 0.05 to ± 0.005 cm^{-1}), and calculated what has stood until now as the most accurate (although not the most extensive) set of neutral ^{7}Li level values, 18 even and ten odd levels. The estimated accuracy for the 16 interferometrically connected levels was ± 0.003 cm^{-1} (0.02 to 0.1 cm^{-1} for the other levels). Later measurements focused on the fine, hyperfine, and isotopic structure intervals. The only reference to improved level values reported remeasurement of five levels ($4s\ ^2S$, $3d\ ^2D_{3/2,5/2}$, $4d\ ^2D_{3/2,5/2}$) by two-photon Doppler-free laser spectroscopy [15]. In 1970 Litzén [16] reported the $4f$-$5g$ infrared transition at 2469 cm^{-1}.

B. Resonance line measurements

Several measurements of the lithium $D1$ and $D2$ resonance line wave numbers have been made using laser-based techniques. In 1986 Fuchs and Rubahn [17] remeasured the D lines with respect to calculated frequencies in the X-A band of $^7Li_2$ using laser-induced fluorescence (LIF). However, their values disagree by 10 cm^{-1} from accepted values. More recently Windholz and Umfer [18] reported results using a laser-excited atomic beam coupled with a wavemeter. Their values were in disagreement with Ref. [10] and claimed a slightly smaller uncertainty. Very recently Sansonetti *et al.* [19] published values based upon frequency modulation spectroscopy. The latter have the highest accuracy yet attained for these spectral lines.

C. Isotope shifts

The isotope shifts for the whole spectrum, both calculated and experimental, were well summarized in Ref. [7]. Measurements of the resonance line isotope shifts through 1990 were summarized by Windholz *et al.* [20]. There are more recent experimental [19] and theoretical [21] results for the resonance line isotope shifts.

D. Rydberg series

Rydberg series wave numbers, reported first in 1910 [12], have not been systematically remeasured since reported in 1930 [22]. Precise measurements of some Rydberg series differences have been made. These include the measurements of d-f and d-g intervals ($n=7$ to 11) [23], and some intervals in the s and p series, in both ^{6}Li and ^{7}Li in the range of $n=18$ to 40 [24]. We used these intervals along with other data to predict splittings for some unresolved doublets as described below. Very recently the $n=10$, g to h and h to i fine structure intervals have been measured to an accuracy of 10 parts per million [25].

E. Series limit and quantum defects

The series limit analysis by Johansson [10] used the measurements of Meissner, Mundie and Stelson [9] for the four lowest ^2D terms. This gave the value 43 487.150 cm^{-1} "which is thought to be correct within 5 mK" (1 mK = 0.001 cm^{-1}) [10]. Quantum defect formulas for ^2S, ^2P, ^2D, and ^2F series were calculated. Using that limit value, Goy *et al.* [24] reported precise values of some quantum defects in the s and p Rydberg levels of both ^{6}Li and ^{7}Li, with n ranging from 18 to 40.

TABLE I. Fine structure splittings for ^{6}Li and ^{7}Li. These are the literature values with the highest reported accuracy in each case.

State	Splitting (MHz)	Method[a]	Reference
	^{6}Li		
$2p\ ^2P^o$	10 050.22(22)	AB-LC	[35]
$3p\ ^2P^o$	2 882.70(15)	AB-LC	[36]
$3d\ ^2D$	1 081.58(31)	BF-QB	[37]
$4d\ ^2D$	455.25(37)	BF-QB	[37]
$5d\ ^2D$	232.57(16)	BF-QB	[37]
$6d\ ^2D$	134.67(12)	BF-QB	[37]
$7d\ ^2D$	84.95(14)	BF-QB	[37]
	^{7}Li		
$2p\ ^2P^o$	10 053.184(58)	AB-LC	[38]
$3p\ ^2P^o$	2 882.903(18)	AB-LC	[36]
$4p\ ^2P^o$	1 199.65(11)	AB-LC	[36]
$5p\ ^2P^o$	625	interpolation	
$6p\ ^2P^o$	360	interpolation	
$18p\ ^2P^o$	11.5(8)	AB-DR	[24]
$21p\ ^2P^o$	8.2(1.0)	AB-DR	[24]
$23p\ ^2P^o$	5.7(3)	AB-DR	[24]
$24p\ ^2P^o$	5.6(4)	AB-DR	[24]
$25p\ ^2P^o$	5.0(5)	AB-DR	[24]
$29p\ ^2P^o$	3.2(2)	AB-DR	[24]
$30p\ ^2P^o$	2.6(5)	AB-DR	[24]
$35p\ ^2P^o$	2.3(4)	AB-DR	[24]
$8d\ ^2D$	56.97(60)	AB-OD	[23]
$9d\ ^2D$	40.04(60)	AB-OD	[23]
$10d\ ^2D$	28.6(1.0)	AB-OD	[23]
$4f\ ^2F^o$	226	extrapolation	
$5f\ ^2F^o$	116	extrapolation	
$6f\ ^2F^o$	67	extrapolation	
$7f\ ^2F^o$	41.99(80)	AB-OD	[23]
$8f\ ^2F^o$	28.05(60)	AB-OD	[23]
$9f\ ^2F^o$	19.86(60)	AB-OD	[23]
$10f\ ^2F^o$	13.6(1.5)	AB-OD	[23]
$5g\ ^2G$	70	extrapolation	
$8g\ ^2G$	17.0(1.2)	AB-OD	[23]
$9g\ ^2G$	12.1(2.0)	AB-OD	[23]

[a]The symbols for method identify the type of source used and indicate in general the type of spectroscopy or detection method. Some symbols pertain to Table II as well. *Sources*: AB, atomic beam; BF, beam foil; HP, heat pipe. *Spectroscopy and detection methods*: DR, double resonance; LC, level crossing; LS, laser spectroscopy; MR, magnetic resonance; OD, optical detection; QB, quantum beats.

III. EXPERIMENT

A. Sources

Two types of lithium hollow cathode emission sources were used in our study. The first were sealed commercial

TABLE II. Hyperfine structure splittings and constants for $2s$, $3s$, $4s$, and $2p$ levels of ^{6}Li and ^{7}Li. These are the literature values with the highest reported accuracy in each case.

State	Splitting (MHz)	A (MHz)	B (MHz)	Method[a]	Reference
		^{6}Li			
$2s\ ^2S_{1/2}$	228.205 259(3)	152.136 840 7(20)		AB-MR	[39]
$3s\ ^2S_{1/2}$	51(20)	34(13)		HP-LS	[7]
$4s\ ^2S_{1/2}$	19.7(2.0)	13.1(1.3)		AB-LS	[40]
$2p\ ^2P^o_{1/2}$		17.375(18)		AB-LC	[41]
$2p\ ^2P^o_{3/2}$		−1.155(8)	−0.10(14)	AB-LC	[41]
		^{7}Li			
$2s\ ^2S_{1/2}$	803.504 086 6(10)	401.752 043 3(5)		AB-MR	[39]
$3s\ ^2S_{1/2}$	189.36(44)	94.68(22)		AB-LS	[8]
$4s\ ^2S_{1/2}$	73.2(8.0)	36.4(4.0)		AB-LS	[40]
$2p\ ^2P^o_{1/2}$		45.914(25)		AB-LC	[38]
$2p\ ^2P^o_{3/2}$		−3.055(14)	−0.221(29)	AB-LC	[38]

[a]See Table I footnote.

hollow cathodes with neon or argon fill gas, operated at currents of 3–15 mA, with isotopic purities of 99.99% ^{7}Li or 98.7–99.3% ^{6}Li. The second were demountable hollow cathodes, operated with less than 1 torr of neon, neon plus argon, argon, or helium at currents 0.6–0.9 A, with isotopic purities of 92.5% ^{7}Li (natural abundance) or 95% ^{6}Li.

For the 670-nm resonance lines, we used the sealed commercial hollow cathode units commonly used for spectrochemistry. Self-reversal of the resonance lines was negligible only at the lowest currents (3 mA). Using a model described in Sec. III C, we extracted a Li linewidth of 0.090 cm^{-1} from the 3-mA measurements, corresponding to a Doppler temperature of 500 K.

The most complete lithium spectra were obtained from the demountable hollow cathodes described in detail elsewhere [26]. Our unit differed in the cathode design and the windows. A calcium fluoride lens was used in place of one window to image the cathode on the entrance aperture of the spectrometer, while the other window was tipped about 10° from the optic axis to reject reflections of the hot cathode wall. The cathode itself was modeled after that first used by Risberg [27] and later used for lithium by Johansson [10]. It was an iron tube (25 mm long, 19 mm outside diameter with 2.5 mm wall) closed at both ends with a welded iron plate 2.5 mm thick. A centered 6-mm hole in each plate provided a port for viewing the emission. The through hole greatly reduced blackbody radiation during infrared measurements, was convenient for optical alignment, and the assembly served as a reservoir for liquid lithium during operation. This cathode was loaded with pieces of either natural or enriched lithium, and operated with neon, argon, helium, or various mixtures as fill gas, at operating currents between 0.6 and 0.9 A. The high currents were required to obtain good excitation, but led to significant Stark effect of some high-lying levels. Even at the high currents, emission lines starting on levels above $n=6$ were not excited significantly.

B. Spectra

All spectra were obtained with the NSO 1-m FTS [28] using several different beamsplitter and detector combinations. Most spectra were the result of about 1 h of integration. Resolution varied from 0.01 to 0.04 cm^{-1} from the infrared to ultraviolet (1800–31 000 cm^{-1}). Reductions were performed using codes specifically designed for Fourier-transform spectra [29].

Accurate wave numbers of argon [30], neon [31], and iron [32] were used to provide small corrections to the spectra. Uncertainties for the lithium lines were first estimated by using a figure of merit for the best accuracy obtainable from FT data: the full-width-at-half-maximum linewidth divided by twice the signal-to-noise ratio [33]. They were then revised for some lines depending on the evidence for Stark effect, record-to-record reproducibility, and the residual of the computed fits to the unresolved line structures, a procedure which is described below.

Excitation temperatures were determined from the Doppler widths of transitions between low-lying excited states, those least susceptible to Stark effect. Excitation temperatures for the high-current sources ranged from 750 to 1500 K.

C. Data analysis

A common problem in high-resolution spectra is extracting information from components which partially overlap, even though some information is known about the intervals of the components. We used a least-squares method of fitting experimentally observed line shapes to extract wave-number values [34]. The method uses a mathematical model of overlapping lines based on the details of the transitions involved. The lithium version of this code, named LILSQ, ignored hyperfine splittings (except for transitions to $3s$ and $4s$) and was used for all transitions except the resonance line. Relative intensities of component lines were fixed at theoretical values. In this model, it is important to set the ratio of the Doppler widths ^{6}Li:^{7}Li to $(7/6)^{1/2}$.

Many known fine structure splittings were not resolved in our experiment. As input to the LILSQ program we used known splittings where these had been measured. Measured splittings with the highest claimed accuracy [23,24,35–38] are shown in Table I. Where there have been multiple mea-

TABLE III. New ^{6}Li and ^{7}Li wave-number and isotope shift measurements.

Intensity	Comment[a]	^{6}Li σ[b] (cm^{-1})	^{7}Li σ (cm^{-1})	Uncertainty (cm^{-1})	IS[c] (cm^{-1})	Classification Lower level	Classification Upper level
145	New L, IS	1 829.663	1 829.668	0.002	0.006	$4p\ ^2P^o_{3/2}-5s\ ^2S_{1/2}$	
80		1 829.703	1 829.708			1/2	1/2
		2 392.324	2 392.365			$4d\ ^2D_{3/2}-5p\ ^2P^o_{1/2}$	
18	New L, IS	2 392.330	2 392.370	0.002	0.040	5/2	3/2
		2 392.345	2 392.386			3/2	3/2
		2 466.488	2 466.542			$4f\ ^2F^o_{7/2}-5d\ ^2D_{3/2}$	
2	Asym red	2 466.488	2 466.542	0.005	0.054	7/2	5/2
	New L, IS	2 466.496	2 466.549			5/2	5/2
33	Forbidden	2 469.15	2 469.16	0.10		4f−5f	
		2 469.58	2 469.60			$4f\ ^2F^o_{7/2}-5g\ ^2G_{7/2}$	
360	Asym blue	2 469.58	2 469.60	0.05	0.03	7/2	9/2
	New IS	2 469.58	2 469.61			5/2	7/2
		2 474.101	2 474.147			$4d\ ^2D_{5/2}-5f\ ^2F^o_{5/2}$	
120	Asym red	2 474.105	2 474.151	0.010	0.046	5/2	7/2
	New L, IS	2 474.116	2 474.162			3/2	5/2
15	Forbidden	2 474.62	2 474.65	0.10		4d−5g	
		2 625.040	2 625.064			$4p\ ^2P^o_{3/2}-5d\ ^2D_{3/2}$	
65	New L, IS	2 625.048	2 625.072	0.003	0.024	3/2	5/2
		2 625.080	2 625.104			1/2	3/2
10	New L, IS	3 517.760	3 517.792	0.003	0.032	$4p\ ^2P^o_{3/2}-6s\ ^2S_{1/2}$	
		3 517.800	3 517.832			1/2	1/2
20 500	New IS	3 719.3626	3 719.4569	0.0010	0.0943	$3s\ ^2S_{1/2}-3p\ ^2P^o_{1/2}$	
36 200		3 719.4593	3 719.5536			1/2	3/2
		3 767.886	3 767.944			$4d\ ^2D_{5/2}-6p\ ^2P^o_{3/2}$	
1	New L, IS	3 767.889	3 767.947	0.010	0.058	3/2	1/2
		3 767.901	3 767.959			3/2	3/2
		3 967.351	3 967.419			$4p\ ^2P^o_{3/2}-6d\ ^2D_{3/2}$	
5	Asym red	3 967.355	3 967.423	0.020	0.068	3/2	5/2
	New L, IS	3 967.391	3 967.459			1/2	3/2
4 070	New IS	4 086.3708	4 086.3835	0.0010	0.0127	$3p\ ^2P^o_{3/2}-4s\ ^2S_{1/2}$	
2 250		4 086.4670	4 086.4797			1/2	1/2
		5 186.6197	5 186.7037			$3d\ ^2D_{3/2}-4p\ ^2P^o_{1/2}$	
4 300	New IS	5 186.6236	5 186.7076	0.0010	0.0840	5/2	3/2
		5 186.6597	5 186.7437			3/2	3/2
		5 345.174	5 345.242			$3d\ ^2D_{5/2}-4f\ ^2F^o_{5/2}$	
12 000	New IS	5 345.181	5 345.250	0.003	0.068	5/2	7/2
		5 345.210	5 345.278			3/2	5/2

TABLE III. (*Continued*).

Intensity	Comment[a]	^{6}Li σ[b] (cm^{-1})	^{7}Li σ (cm^{-1})	Uncertainty (cm^{-1})	IS[c] (cm^{-1})	Classification Lower level	Classification Upper level
		5 697.647	5 697.686			$3p\ ^2P^o_{3/2}$	$-4d\ ^2D_{3/2}$
3 830	New IS	5 697.663	5 697.701	0.002	0.038	3/2	5/2
2 370		5 697.744	5 697.782			1/2	3/2
120	New IS	7 373.7550	7 373.8129	0.0010	0.0579	$3p\ ^2P^o_{3/2}$	$-5s\ ^2S_{1/2}$
65		7 373.8512	7 373.9091			1/2	1/2
		7 732.518	7 732.630			$3d\ ^2D_{5/2}$	$-5p\ ^2P^o_{3/2}$
16	New L, IS	7 732.533	7 732.644	0.003	0.111	3/2	1/2
		7 732.554	7 732.666			3/2	3/2
		7 814.30	7 814.41			$3d\ ^2D_{5/2}$	$-5f\ ^2F^o_{5/2}$
230	Asym red	7 814.30	7 814.42	0.03	0.11	5/2	7/2
	New IS	7 814.34	7 814.45			3/2	5/2
40	Forbidden	7 814.82	7 815.00	0.10		3d	−5g
		8 169.1321	8 169.2071			$3p\ ^2P^o_{3/2}$	$-5d\ ^2D_{3/2}$
160	New IS	8 169.1399	8 169.2149	0.0015	0.0750	3/2	5/2
		8 169.2283	8 169.3033			1/2	3/2
10	New IS	9 061.853	9 061.934	0.006	0.080	$3p\ ^2P^o_{3/2}$	$-6s\ ^2S_{1/2}$
		9 061.950	9 062.030			1/2	1/2
10	Blend[d]	9 155.69	9 155.81	0.10		3d	−6f, 6g
		9 511.453	9 511.554			$3p\ ^2P^o_{3/2}$	$-6d\ ^2D_{3/2}$
10	Asym red	9 511.457	9 511.559	0.020	0.101	3/2	5/2
	New IS	9 511.549	9 511.650			1/2	3/2
3.42×10^6		12 302.0799	12 302.1110	0.0010	0.0311	$2p\ ^2P^o_{3/2}$	$-3s\ ^2S_{1/2}$
1.73×10^6		12 302.4152	12 302.4463			1/2	1/2
1.62×10^{10}		14 903.2973	14 903.6483	0.0005	0.3511	$2s\ ^2S_{1/2}$	$-2p\ ^2P^o_{1/2}$
3.23×10^{10}		14 903.6327	14 903.9838			1/2	3/2
		16 378.9728	16 379.0661	0.0015	0.0932	$2p\ ^2P^o_{3/2}$	$-3d\ ^2D_{3/2}$
3.91×10^6		16 379.0089	16 379.1021			3/2	5/2
2.31×10^6		16 379.3081	16 379.4014			1/2	3/2
55 000		20 107.9107	20 108.0490	0.0010	0.1383	$2p\ ^2P^o_{3/2}$	$-4s\ ^2S_{1/2}$
27 800		20 108.2460	20 108.3843			1/2	1/2
		21 719.1916	21 719.3539			$2p\ ^2P^o_{3/2}$	$-4d\ ^2D_{3/2}$
237 000		21 719.2067	21 719.3691	0.0015	0.1624	3/2	5/2
125 000		21 719.5268	21 719.6893			1/2	3/2
3 110		23 395.2974	23 395.4805	0.0015	0.1831	$2p\ ^2P^o_{3/2}$	$-5s\ ^2S_{1/2}$
1 580		23 395.6326	23 395.8158			1/2	1/2
		24 190.688	24 190.886			$2p\ ^2P^o_{3/2}$	$-5d\ ^2D_{3/2}$
14 250		24 190.695	24 190.894	0.002	0.198	3/2	5/2
7 570		24 191.023	24 191.221			1/2	3/2

TABLE III. (*Continued*).

Intensity	Comment[a]	^{6}Li σ[b] (cm^{-1})	^{7}Li σ (cm^{-1})	Uncertainty (cm^{-1})	IS[c] (cm^{-1})	Classification Lower level	Classification Upper level
270	New IS	25 083.408	25 083.610	0.010	0.201	$2p\ ^2P^o_{3/2}-6s\ ^2S_{1/2}$	
140		25 083.744	25 083.945			1/2	1/2
		25 533.03	25 533.25			$2p\ ^2P^o_{3/2}-6d\ ^2D_{3/2}$	
1 090	New IS	25 533.03	25 533.26	0.02	0.22	3/2	5/2
575		25 533.36	25 533.59			1/2	3/2
14 660		30 925.08	30 925.55	0.02	0.48	$2s\ ^2S_{1/2}-3p\ ^2P^o_{1/2}$	
		30 925.17	30 925.65			1/2	3/2

[a]Lines observed for the first time and isotope shifts measured for the first time are labeled as "New L, IS," respectively.

[b]The following lines were listed in Ref. [10] but not observed by us: 9964.57, 10 042.36, 10 320.95, 10 489.50, 10 661.80, 10 846.16, 10 849.35, 11 206.26, 11 809.61 cm^{-1}. The following lines were observed but with very poor signal to noise: 4498, 9108 cm^{-1}.

[c]Isotope shift values were determined by differencing the wave-number values before rounding.

[d]The profile appears to be a blend of $3d$-$6f$ and $3d$-$6g$. The wave numbers are estimates.

surements, those with the highest stated accuracy were used. For $n>3$ nd $l>1$ the splittings in ^{6}Li and ^{7}Li were assumed to be identical. We also required some splittings which had not been measured, namely $5p$, $6p$, $4f$, $5f$, $6f$, and $5g$. These were estimated by using an $(n^*)^{-3}$ interpolation between known values for the p series, and an extrapolation below the known values for the f and g series. Our predicted values are also given in Table I. Hyperfine structure constants used in the analysis of the resonance lines and a few other $3s$ and $4s$ transitions [7,8,38–41] are given in Table II.

IV. RESULTS

A. Wave-number measurements

Our wave-number measurements for both isotopes are contained in Table III. Thirty-four lines were observed, nine in the infrared which had previously not been observed. Twenty-two new isotope shifts were also measured. Three dipole-forbidden lines were excited in the high-current sources.

The first column of Table III contains the relative peak intensities. For well-resolved fine structure components, the intensity is given separately for each peak. Otherwise we give the peak intensity of the unresolved features. Because the spectra were taken from scans over different spectral regions, we scaled intensities from region to region. As a reference we used a standard tungsten filament lamp, scans of which were taken just before or after each run over the same wave-number interval. These provided the baseline for adjusting the lithium intensities. The second column contains comments about the line and an indication of the newly observed lines and first-time isotope shift measurements.

The next four columns contain the ^{6}Li and ^{7}Li wave numbers, respectively, their uncertainties determined as described above, and the $\sigma(^7\text{Li})$-$\sigma(^6\text{Li})$ isotope shift. The uncertainty for a given line applies to both isotopes because the same line in both isotopes had very similar signal to noise and linewidth. Twenty of the 34 lines were assigned uncertainties between ± 0.001 and ± 0.005 cm^{-1}.

The last column in Table III contains the line classification. Note that what was actually observed was often a blend of the two or three components for each transition. The $3s$-$4p$ transition was not observed, nor was it excited in the work reported in Ref. [10]. This is a Cooper minimum [42], which in Li I occurs at $3s$-$4p$ in the $3s$-np $n\geqslant 3$ series (see the corresponding open circle in Fig. 1).

The average difference between Johansson's [10] and our infrared measurements is about 0.01 cm^{-1}. There are larger, systematic differences with the previous ultraviolet measurements of Meissner, Mundie, and Stelson [9] corrected by Johansson [10]. These differences range from -0.005 cm^{-1} (the minus sign means our values are lower in wave number) for 16 379 to -0.03 cm^{-1} for 25 533 cm^{-1}, and are larger for the $2p$-nd transitions than for the $2p$-ns transitions. If one assumes that Meissner's measurements with the atomic beam are the least susceptible to Stark effect, these shifts are consistent with a Stark-effect-induced depression (in our Risberg-type hollow cathode) of the higher nd

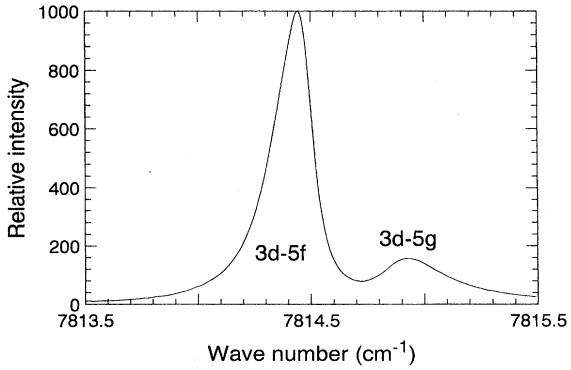

FIG. 2. The $3d$-$5f$ transition from a high-current hollow cathode. The forbidden $3d$-$5g$ line is on the high wave-number side.

TABLE IV. ^{6}Li and ^{7}Li level values, calculated from the center of gravity of the hyperfine structure of the ground state. Uncertainties apply to both sets of level values and the level isotope shift except where a different uncertainty is explicitly stated in parentheses.

Designation	^{6}Li level value (cm^{-1})	Uncertainty (cm^{-1})	^{7}Li level value (cm^{-1})	Level isotope shift (cm^{-1})
$2s\ ^2S_{1/2}$	0.000 0	0.000 0	0.000 0	0.000 0
$3s\ ^2S_{1/2}$	27 205.712 9	0.001 0	27 206.095 2	0.382 3
$4s\ ^2S_{1/2}$	35 011.543 2	0.001 0	35 012.032 6	0.489 4
$5s\ ^2S_{1/2}$	38 298.928 3	0.001 0	38 299.462 7	0.534 4
$6s\ ^2S_{1/2}$	39 987.027	0.004	39 987.586(3)	0.559
$2p\ ^2P^o_{1/2}$ [a]	14 903.296 792	0.000 023	14 903.648 130(14)	0.351 338(21)
$^2P^o_{3/2}$ [a]	14 903.632 116	0.000 018	14 903.983 468(14)	0.351 352(15)
$3p\ ^2P^o_{1/2}$	30 925.076 4	0.001 0	30 925.553 0	0.476 6
$^2P^o_{3/2}$	30 925.172 8	0.001 0	30 925.649 4	
$4p\ ^2P^o_{1/2}$	36 469.225 9	0.001 5	36 469.754 2	0.528 3
$^2P^o_{3/2}$	36 469.266 0	0.001 5	36 469.794 3	
$5p\ ^2P^o_{1/2}$	39 015.143 9[b]	0.002 0	39 015.698 8[b]	0.554 9
$^2P^o_{3/2}$	39 015.164 9	0.002 0	39 015.719 9	
$6p\ ^2P^o_{1/2}$	40 390.711[b]	0.010	40 391.283[b]	0.572
$^2P^o_{3/2}$	40 390.723	0.010	40 391.295	
$3d\ ^2D_{3/2}$	31 282.606 2	0.001 5	31 283.050 5(10)	0.444 3
$^2D_{5/2}$	31 282.642 3	0.001 5	31 283.086 6(10)	
$4d\ ^2D_{3/2}$	36 622.821 7	0.001 5	36 623.336 0(10)	0.514 3
$^2D_{5/2}$	36 622.836 8	0.001 5	36 623.351 1(10)	
$5d\ ^2D_{3/2}$	39 094.310	0.010	39 094.861	0.551
$^2D_{5/2}$	39 094.318	0.010	39 094.869	
$6d\ ^2D_{3/2,5/2}$	40 436.633	0.020	40 437.220	0.587
$4f\ ^2F^o_{5/2}$	36 627.816[b]	0.003	36 628.329[b]	0.513
$^2F^o_{7/2}$	36 627.824	0.003	36 628.336	
$5f\ ^2F^o_{5/2}$	39 096.940[b]	0.015	39 097.499[b]	0.559
$^2F^o_{7/2}$	39 096.943	0.015	39 097.503	
$6f\ ^2F^o_{5/2,7/2}$	40 438.33	0.05	40 438.90	0.57
$5g\ ^2G_{7/2,9/2}$	39 097.403	0.006	39 097.941	0.54

[a]Values from Ref. [19].

[b]Splittings from Table I.

levels (except for $3d$ [20,43]) as compared with the ns levels.

The full description of the lithium resonance lines is complex because two isotopes with natural abundance have an isotope shift comparable in magnitude to the fine structure splitting. In addition there are appreciable hyperfine splittings; the nuclear spin is 1 for ^{6}Li and $\frac{3}{2}$ for ^{7}Li. A second version of the line profile fitting code, LILSQ, was used for the resonance lines. It used the fine structure splittings in Table I and the hyperfine date in Table II.

The resonance line uncertainties, estimated from the full-width-at-half-maximum linewidth divided by twice the signal-to-noise ratio, were ± 0.0005 cm^{-1}. Our values are 0.0002–0.0005 cm^{-1} higher than the results for the centers of gravity of the hyperfine patterns of the four lines presented in Ref. [19]. Considering the differences in sources and experiments, we consider that good agreement. In contrast, the values for the comparable features presented in Ref. [18] are 0.010 cm^{-1} lower than either our or the values of Ref. [19]. Finally, the $D1$ and $D2$ line values presented in Ref. [10] are 0.006 cm^{-1} higher than our values. We have included our values in Table III instead of the more accurate ones of Ref. [19] because of the possibility that the values are source dependent.

The linewidths and asymmetries of some features and forbidden transitions indicate that some high levels were perturbed by Stark effect in the high-current Risberg-type source. A comparison of linewidths for several s-p transitions showed them to scale like a Doppler width as a function of wave number. Other transitions, especially those involving high d states, or the f and g states, had asymmetric profiles and linewidths much larger than Doppler. In the case of three transitions, we saw dipole-forbidden satellites at the calculated positions. All involved mixing of $5f$ and $5g$ whose center-of-gravity spacing is 0.43 cm^{-1}. The allowed and forbidden pairs were $4f$-$5g$ ($4f$-$5f$), $4d$-$5f$ ($4d$-$5g$), and $3d$-$5f$ ($3d$-$5g$). The latter is illustrated in Fig. 2. Hence in some cases the wave numbers we report, though accurate, may not be those which would be observed in field-free conditions. The infrared spectrum had been measured earlier with a hollow cathode operated under similar conditions [10], but without sufficient resolution to observe these effects.

We checked for water vapor absorption in the continuum generated by the tungsten lamp. The only significant overlap

TABLE V. Comparison of experimental, extrapolated, and theoretical specific mass shifts in ^{6,7}Li. The previous values cited for comparison are the literature values with the highest reported accuracy in each case.

Level	Specific mass shift in ^{6,7}Li (MHz)			
	This work	Previous experiment	Extrapolated [7]	Theory [48]
$2s$		+1111(6) [49]		[a]
$3s$	+260(30)	+276(26) [7]		+230
$4s$	+94(30)	+111(12) [49]		+88
$5s$	+27(30)	−62(131) [47]	+53	+42
$6s$	−46(120)		+29	+24
$2p$ 1/2	−3603(15)	−3610.0(6) [19]		[a]
$2p$ 3/2	−3603(15)	−3610.3(5) [19]		[a]
$3p$	−1116(30)	−1105(8) [7]		−1034
$4p$	−504(45)		−469	−442
$5p$	−308(60)		−240	−227
$3d$	−11(45)	0(6) [49]		
$4d$	−24(45)	0(6) [49]		
$4f$	+17(90)			

[a]Many theoretical results. See Ref. [7] for details.

with a lithium line occurred for 5345 cm^{-1}. When we eliminated the water vapor profile from the lithium spectrum and then performed a line fitting analysis, the ^{6}Li wave number shifted 0.0004 cm^{-1} and the ^{7}Li wave number was shifted 0.0002 cm^{-1}, both to smaller values. The changes are an order of magnitude smaller than the uncertainty of 0.003 cm^{-1}, hence are negligible.

B. Level values and level isotope shifts

We calculated level values using our data, except that we used the more accurate results of Ref. [19] for the resonance lines. The level values and level isotope shifts are contained in Table IV. Except for $2p$, where there is some evidence that the isotope shift is slightly different for different J values of the doublet [19], only one level isotope shift is given per doublet.

The code [44,45] used for the calculation of the level values uses a matrix inversion algorithm to perform a weighted least-squares fit of level values to transition wave numbers. The uncertainties are estimates based on the fit and the uncertainty of the underlying wave-number data. The higher d levels and the f and g levels are almost certainly perturbed by Stark effect, but the isotope shift differences are probably less affected.

C. Specific mass shifts

Specific mass shifts (SMS) are important for many applications. They are a diagnostic for electron correlation effects [6] and exchange effects between core and Rydberg electrons [24]. The traditional technique of using isotope shifts to obtain information about nuclear charge distributions depends on being able to separate the specific and field effects. The procedure for heavy elements is to calculate the SMS and subtract it and the normal (also called Bohr) mass shift to obtain the field (also called volume) shift which is nucleus dependent. Theorists use lithium as a test case for the SMS calculations because the field shift contribution is negligible [7]. A good example is a 1986 calculation which used a 352-term Hylleraas-type wave function [46]. That reference also refers to other previous theoretical approaches. Hughes [47] had made the first comparison of calculated and experimental SMS for lithium in 1955.

We assume, as was done in Ref. [7], that the residual level isotope shift (RLIS) is equal to the SMS for lithium. The RLIS is the level isotope shift less the Bohr and $2s$ shifts. We have also adopted the approach of Ref. [7] and give values for the shifts of individual levels rather than transitions. Then the expression for the Bohr mass shift (BMS) for lithium levels is

$$\delta E_{BMS} = 1.301\ 030(4) \times 10^{-5} E,$$

where E is the level value in cm^{-1}. The resulting specific mass shifts are in Table V. Because of their small values only isotope shifts with an uncertainty less than ± 0.005 cm^{-1} were used. For comparison, previous best measurements, extrapolated values, and some theoretical results [7,19,47–49] are included in the table.

V. CONCLUSION

Using high- and low-current hollow cathode sources and Fourier-transform spectrometry we have made measurements in both ^{7}Li and ^{6}Li. Data were obtained on 34 lines from 1829 to 30 925 cm^{-1} including nine infrared lines previously not measured. The energy levels have been recalculated. We also measured 22 new isotope shifts, and added specific mass shifts for five levels.

ACKNOWLEDGMENTS

We gratefully acknowledge the support of the National Solar Observatory in making their facilities available for this work.

[1] D. K. McKenzie and G. W. F. Drake, Phys. Rev. A **44**, R6973 (1991).
[2] M. Tong, P. Jönsson, and C. Froese Fischer, Phys. Scr. **48**, 446 (1993).
[3] R. J. Drachman and A. K. Bhatia, Phys. Rev. A **51**, 2926 (1995).
[4] A. I. Boothroyd, I.-J. Sackmann, and W. A. Fowler, Astrophys. J. **377**, 318 (1991).
[5] V. V. Smith, D. L. Lambert, and P. E. Nissen, Astrophys. J. **408**, 262 (1993).
[6] W. H. King, *Isotope Shifts in Atomic Spectra* (Plenum, New York, 1984), pp. 27–30.
[7] C. Vadla, O. Obrebski, and K. Niemax, Opt. Commun. **63**, 288 (1987).
[8] G. D. Stevens, C.-H. Iu, S. Williams, T. Bergeman, and H. Metcalf, Phys. Rev. A **51**, 2866 (1995).
[9] K. W. Meissner, L. G. Mundie, and P. H. Stelson, Phys. Rev. **74**, 932 (1984); **75**, 891(E) (1949).
[10] I. Johansson, Ark. Fys. **15**, 169 (1959).
[11] A. M. Cantù, W. H. Parkinson, G. Tondello, and G. P. Tozzi, J. Opt. Soc. Am. **67**, 1030 (1977).
[12] P. V. Bevan, Proc. R. Soc. London, Ser. A **83**, 43 (1910).
[13] P. Zeeman, Phys. Z. **14**, 914 (1913).
[14] C. E. Moore, *Atomic Energy Levels Vol. 1*, Natl. Bur. Stand. (U.S.) No. NSRDS-NBS 35 (U.S. GPO, Washington, DC, 1971).
[15] C.-J. Lorenzen and K. Niemax, Phys. Scr. **27**, 300 (1983).
[16] U. Litzén, Phys. Scr. **1**, 253 (1970).
[17] M. Fuchs and H.-G. Rubahn, Z. Phys. D **2**, 253 (1986).
[18] L. Windholz and C. Umfer, Z. Phys. D **29**, 121 (1994).
[19] C. J. Sansonetti, B. Richou, R. Engleman, Jr., and L. J. Radziemski, Phys. Rev. A **52**, 2682 (1995).
[20] L. Windholz, H. Jäger, M. Musso, and G. Zerza, Z. Phys. D **16**, 41 (1990).
[21] G. W. F. Drake (private communication).
[22] R. W. France, Proc. R. Soc. London, Ser. A **129**, 354 (1930).
[23] W. E. Cooke, T. F. Gallagher, R. M. Hill, and S. A. Edelstein, Phys. Rev. A **16**, 1141 (1977).
[24] P. Goy, J. Liang, M. Gross, and S. Haroche, Phys. Rev. A **34**, 2889 (1986).
[25] N. E. Rothery, C. H. Storry, and E. A. Hessels, Phys. Rev. A **51**, 2919 (1995).
[26] R. A. Keller, B. E. Warner, E. F. Zalewski, P. Dyer, R. Engleman, Jr., and B. A. Palmer, J. Phys. (Paris) Colloq. **44**, C7-23 (1983).
[27] P. Risberg, Ark. Fys. **10**, 583 (1956).
[28] J. W. Brault, J. Opt. Soc. Am. **66**, 1081 (1976).
[29] J. W. Brault and M. C. Abrams, Opt. Soc. Am. Tech. Dig. Ser. **6**, 118 (1989).
[30] G. Norlén, Phys. Scr. **8**, 249 (1973).
[31] B. A. Palmer and R. Engleman, Jr., Los Alamos National Laboratory Report No. LA-9615, Appendix B, 1983 (unpublished).
[32] G. Nave, R. C. M. Learner, J. E. Murray, A. P. Thorne, and J. W. Brault, J. Phys. (France) II **2**, 913 (1992).
[33] J. Brault, Microchim. Acta **III**, 215 (1987).
[34] R. Engleman, Jr. and J. W. Brault, Opt. Soc. Am. Tech. Dig. Ser. **4**, 45 (1995).
[35] K. C. Brog, T. G. Eck, and H. Wieder, Phys. Rev. **153**, 91 (1967).
[36] R. C. Isler, S. Marcus, and R. Novick, Phys. Rev. **187**, 66 (1969).
[37] J. Wangler, L. Henke, W. Wittmann, H. J. Plöhn, and H. J. Andrä, Z. Phys. A **299**, 23 (1981).
[38] H. Orth, H. Ackermann, and E. W. Otten, Z. Phys. A **273**, 221 (1975).
[39] A. Beckmann, K. D. Böklen, and D. Elke, Z. Phys. **270**, 173 (1974).
[40] J. Kowalski, R. Neumann, H. Suhr, K. Winkler, and G. zu Putlitz, Z. Phys. A **287**, 247 (1978).
[41] E. Arimondo, M. Inguscio, and P. Violino, Rev. Mod. Phys. **49**, 31 (1977).
[42] U. Fano and A. R. P. Rau, *Atomic Collisions and Spectra* (Academic, New York, 1986), p. 34.
[43] S. I. Themelis and C. A. Nicolaides, Phys. Rev. A **51**, 2801 (1995).
[44] R. Engleman, Jr. and B. A. Palmer, J. Opt. Soc. Am. **70**, 308 (1980).
[45] L. J. Radziemski, K. J. Fisher, D. W. Steinhaus, and A. S. Goldman, Comput. Phys. Commun. **3**, 9 (1972).
[46] F. W. King, Phys. Rev. A **34**, 4543 (1986).
[47] R. H. Hughes, Phys. Rev. **99**, 1837 (1955).
[48] A.-M. Mårtensson and S. Salomonson, J. Phys. B **15**, 2115 (1982).
[49] C.-J. Lorenzen and K. Niemax, J. Phys. B **15**, L139 (1982).